ELECTROMAGNETIC DIFFRACTION BY PLANE REFLECTION DIFFRACTION GRATINGS

R. P. Bocker
A. S. Marathay

Final Report
Prepared for the
National Aeronautics and
Space Administration
Under Contract NAS 5-11456

Optical Sciences Center
University of Arizona
Tucson, Arizona 85721
July 1972

ELECTROMAGNETIC DIFFRACTION BY PLANE REFLECTION DIFFRACTION GRATINGS

R. P. Bocker
A. S. Marathay

Final Report
Prepared for the
National Aeronautics and
Space Administration
Under Contract NAS 5-11456

Optical Sciences Center
University of Arizona
Tucson, Arizona 85721
July 1972

ABSTRACT

We developed a plane wave theory to study electromagnetic diffraction by plane reflection diffraction gratings of infinite extent. A computer program was written to calculate the energy distribution in the various orders of diffraction for the cases when the electric or magnetic field vectors are parallel to the grating grooves. We ran test cases and compared our results with those found in the literature. Within the region of validity of this theory, our results were in excellent agreement with those in the literature. Energy conservation checks were also made to determine the region of validity of the plane wave theory. The computer program was flexible enough to analyze any grating profile that could be described by a single value function $f(x)$. Within the region of validity the program could be used with confidence.

The computer program was used to investigate the following:

(a) *Polarization Properties of the Diffraction Grating:* For an echelette grating profile, we were able to determine the wavelength at which the grating would completely linearly polarize the light in a prespecified order for any general state of incident polarized light.

(b) *Blaze Properties of the Diffraction Grating:* For a similar echelette grating profile, we determined the wavelength at which the blaze efficiency would be a maximum. Our calculation, which was done for the case when the electric field vector is parallel to the grating grooves, indicated that a blaze efficiency as high as 0.99 in the -1^{st} order could be obtained when the double Woods anomaly condition was satisfied. The wavelength, grating period, and angle of incidence necessary to give the double Woods anomaly condition also satisfied the Bragg condition.

The study was extended to determine what effect an echelette grating profile with rounded edges would have on the blazing properties of the grating. We found that in the worst rounding case, where 50% of the blaze facet is flat, the blaze efficiency of the -1^{st} order had dropped to a value of only 0.91. The rounded edge case is of practical importance because such grating profiles can now be made on a photoresist material using the holographic process with grating periods on the order of 1 μm.

CONTENTS

1. INTRODUCTION

One of the most important optical devices used in spectroscopy to study the frequency composition of light is the diffraction grating. Diffraction gratings consist of an assembly of narrow grooves and are used in either the transmission or the reflection mode. Unlike prisms, with which the incident energy in a given wavelength appears in only one direction, diffraction gratings split the incident beam into a number of diffracted beams that leave the grating at different angles. These diffracted beams are commonly referred to as diffraction orders. The angular distribution of these diffraction orders is given by the well-known grating equation

$$\sin\theta_i + \sin\theta_m = m(\lambda/a) \tag{1.1}$$

where

θ_i = angle of incidence
θ_m = angle of diffraction of order m
m = integer
λ = wavelength of light
a = diffraction grating period.

It is obvious from the grating equation that the zero-order diffracted beam ($m = 0$) is merely a specular reflection off the grating plane. The zero order is also a nondispersive order; that is, the zero-order diffraction angle θ_0 is independent of the wavelength λ. It is for this reason that the zero order is of little interest. Dispersion will occur in orders other than the zero order if they are real. That is, real or homogeneous diffraction orders are those for which the inequality

$$|\sin\theta_m| \leqslant 1 \tag{1.2}$$

is satisfied, which implies

$$-\pi/2 \leqslant \theta_m \leqslant +\pi/2. \tag{1.3}$$

Solving the grating equation for θ_m yields

$$\theta_m(\lambda) = \sin^{-1}[m(\lambda/a) - \sin\theta_i], \tag{1.4}$$

which shows that the diffraction angle θ_m is a function of λ for $m \neq 0$. It is the real dispersive orders that are of physical interest. The grating equation also predicts the occurrence of evanescent orders. That is, for fixed values of a, λ, and θ_i, there are values of $\pm m$ for which the inequality

$$|\sin\theta_m| > 1 \tag{1.5}$$

is satisfied and yields nonphysical angles θ_m. Orders for which the inequality (1.5) is satisfied are commonly referred to as evanescent or inhomogeneous diffraction orders.

The study of diffraction gratings is relatively old and has been the subject of numerous theoretical and experimental investigations. Past calculations based on scalar models of diffraction have yielded unsatisfactory results owing to the fact that diffraction gratings, in general, tend to polarize the diffracted light and to produce energy distributions in the various diffraction orders. These distributions differ as a function of wavelength and angle of incidence for two orthogonal states of polarization, and neither distribution agrees with the predictions based on scalar models. Therefore, in order to take into account the polarization properties of light as well as to properly study the energy distribution properties of diffraction gratings, whether they be conventionally ruled gratings or the new holographic gratings, a rigorous electromagnetic theory must be employed because the interaction of light with a grating is by nature an electromagnetic boundary phenomenon.

A review was made of recently published articles that discuss the rigorous electromagnetic models used to predict energy distributions in the various diffraction orders. Based on this review, a computer program was written to calculate the energy distribution in the various diffraction orders for perfectly conducting, plane periodic reflection gratings of infinite extent. The present computer program can be used successfully only for the analysis of shallow-groove gratings. With this program a detailed analysis of the energy distribution among the various orders can be made based on the inputs of groove profile, grating period, angle of incidence, polarization state, and the wavelength of light. The computer program was used to investigate the polarizing and blaze properties of a diffraction grating with an echelette profile. Recently it was demonstrated that gratings with echelette profiles with slightly rounded edges can be holographically made. The blaze properties of this profile were also investigated. Presented in this report are the results of this investigation.

2. VECTOR DIFFRACTION

With the recent availability of holographic optical gratings[1] and high-resolution, ruled diffraction gratings,[2] a new interest in the solution to the problem of determining the distribution of energy scattered in various orders of diffraction from a grating has arisen. The problem is relatively old and has been the subject of numerous theoretical and experimental investigations. It is well known that past calculations based on scalar models of diffraction[3,4] have yielded unsatisfactory predictions of the distribution of diffracted energy as a function of incidence angle and wavelength. This has occurred because gratings will tend to polarize the diffracted light and produce energy distributions that differ for two orthogonal states of polarization and that do not agree with the predictions based on scalar models.[5]

To take into account the polarization properties of the diffracted light as well as to explain the discrepencies that have resulted between experimental and theoretical predictions based on scalar models, rigorous vector models based on classical electromagnetic theory have recently been developed.[5-10] A rigorous electromagnetic theory must be employed because the interaction of light with a grating is by nature an electromagnetic boundary phenomenon. In fact experiments have shown that the electromagnetic character of light manifests itself predominantly when the grating constant becomes comparable to the wavelength of light that is of interest.[1]

We have reviewed the recently published articles[5-10] that discuss the rigorous electromagnetic models for predicting energy distribution. Based on this review, we have developed a computer program that calculates the energy distribution for perfectly conducting, plane periodic gratings of infinite extent. The theoretical basis for this computer program is the hypothesis that the diffracted field can be represented by a discrete spectrum of plane waves. The problem then is to determine the amplitude coefficients of each of these various discrete diffraction orders based on the boundary conditions on the grating surface that are to be satisfied by the total electromagnetic field. Our mathematical approach parallels that of Meecham [10] although we believe our approach is more easily implemented for computer use.

Because the light incident on a diffraction grating is, in general, either unpolarized or polarized in various ways, the solutions for two orthogonal polarization states are necessary. In the analysis of plane reflection diffraction gratings, it is usually assumed that the incident light is a plane wave with the propagation vector lying in a plane perpendicular to the grooves of the grating. This being the case, it is convenient to consider the two orthogonal polarization cases when the incident electric and magnetic field vectors are parallel to the grating grooves. These two cases are commonly referred to as the transverse electric (TE), also called E-parallel, and transverse magnetic (TM), also called H-parallel, cases, respectively. We now present the underlying theory that forms the basis of our computer program for calculating the energy distribution in the various diffraction orders arising from a perfectly conducting, plane periodic grating of infinite extent.

2.1 Theory

The theoretical bases for this computer program are the assumptions that the incident field is a monochromatic electromagnetic plane wave with the wave propagation vector lying in a plane perpendicular to the grooves of the grating and that the diffracted field can be

represented as a linear combination of plane waves. The problem is to determine the unknown amplitude coefficients associated with each of the plane waves comprising the diffracted field by satisfying the electromagnetic boundary conditions at the surface of the diffraction grating. With a knowledge of the amplitude coefficients, the energy distribution can be readily calculated.

2.1.1 Theory for the TE case

Figure 2.1 depicts the diffraction geometry. The grating profile is described by the equation $y = f(x)$, and has period a. The grooves of the grating are parallel to the z axis.

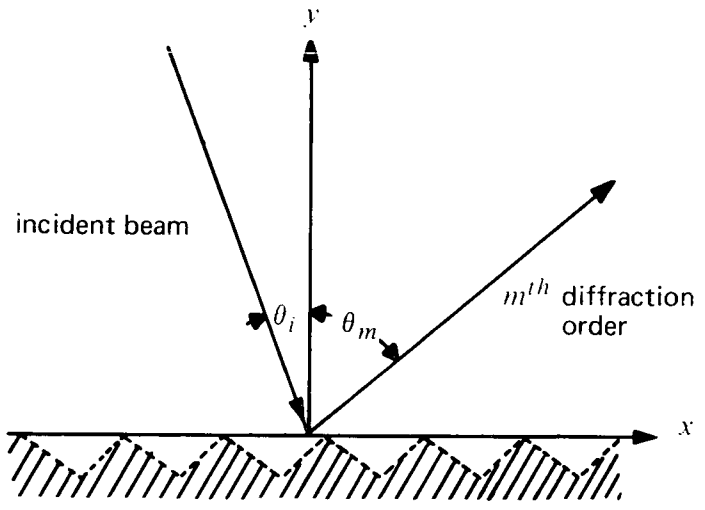

Fig. 2.1. Diffraction grating geometry.

Because the incident field is a monochromatic electromagnetic plane wave with the wave propagation vector lying in the xy plane and the electric field vector parallel to the z axis, then the wave function associated with the incident field is given by

$$\mathbf{E}_i(x,y,z,t) = [0,0,E_{iz}(x,y,z)] \exp(-i\omega t), \tag{2.1}$$

and the time-independent part of the wave function is given by

$$E_{iz}(x,y,z) = E_o \exp(-ikx \sin\theta_i) \exp(-iky \cos\theta_i) \tag{2.2}$$

where k is the wavenumber, ω is the angular frequency, and θ_i is the angle of incidence measured from the $+y$ direction. By symmetry, the diffracted electric field vector will also be parallel to the z axis; that is,

$$\mathbf{E}_d(x,y,z,t) = [0,0,E_{dz}(x,y,z)] \exp(-i\omega t) \tag{2.3}$$

where now

$$E_{dz}(x,y,z) = -\sum_{m=-\infty}^{\infty} A_m \exp(+ikx \sin\theta_m) \exp(iky \cos\theta_m). \tag{2.4}$$

The coefficients A_m are the unknown amplitude coefficients to be determined. The angles θ_m specify the direction of the propagation vectors associated with the various diffraction orders and are determined by the grating equation, which is given by

$$\sin\theta_m + \sin\theta_i = m(\lambda/a) \tag{2.5}$$

where m is an integer, λ is the wavelength, and a is the grating period.

Equation (2.4) represents the plane wave expansion of the diffracted field. It should be noted that only a finite number of the plane wave expansion terms in Eq. (2.4) are associated with real homogeneous plane waves. The remainder of the plane wave expansion terms are associated with evanescent waves. It is the real homogeneous plane waves that are of interest because they are the ones whose energy is actually measured. The evanescent waves are needed to satisfy the boundary condition at the surface of the grating. The boundary condition to be satisfied at the grating surface for the TE case is that the tangential component of the total electric field be identically equal to zero. Mathematically we have

$$E_z(x,y,z)\,|_{y=f(x)} = 0 \tag{2.6}$$

where

$$E_z(x,y,z) = E_{iz}(x,y,z) + E_{dz}(x,y,z). \tag{2.7}$$

Substitution of Eqs. (2.2) and (2.4) into Eq. (2.7) gives

$$E_o \exp(-ikx \sin\theta_i) \exp(-ikf(x) \cos\theta_i) = \sum_{m=-\infty}^{\infty} A_m \exp(+ikx \sin\theta_m) \exp(+ikf(x) \cos\theta_m). \tag{2.8}$$

Without loss of generality we may conveniently let $E_o = 1$.

With the use of the grating equation, Eq. (2.8) can be rewritten in the compact form

$$\psi_i(x) = \sum_{m=-\infty}^{\infty} A_m \exp(+i2\pi mx/a)\psi_m(x) \tag{2.9}$$

where the new functions $\psi_i(x)$ and $\psi_m(x)$ have been defined, for purposes of convenience, by the equations

$$\begin{aligned} \psi_i(x) &= \exp[-ikf(x) \cos\theta_i] \\ \psi_m(x) &= \exp[+ikf(x) \cos\theta_m]. \end{aligned} \tag{2.10}$$

Equation (2.9) is the fundamental equation for the transverse electric case that connects the unknown amplitude coefficients A_m to the wavelength λ, the angle of incidence θ_i, the grating constant a, and the groove profile function $f(x)$. The problem now is to solve for these unknown amplitude coefficients A_m for all values of m. This is generally not possible because the functions contained in the infinite sum of Eq. (2.9) are not, in general, mutually orthogonal. Thus we are forced to find an alternative technique for determining the unknown amplitude coefficients.

The technique we have used is very similar to the one that Meecham[10] has successfully employed. In Meecham's approach he first defines a new function $\chi_i(x)$ by the equation

$$\chi_i(x) = \sum_{m=\min}^{\max} B_m \exp(+i2\pi mx/a)\, \psi_m(x) \tag{2.11}$$

where max and min are finite integers. He then approximates the unknown coefficients A_m by the coefficients B_m for those values of m that are contained in the interval [min,max]. The coefficients B_m are determined by minimizing the mean square error between the functions $\chi_i(x)$ and $\psi_i(x)$. That is, by defining an error ϵ according to the equation

$$\epsilon = (1/a) \int_0^a |\chi_i(x) - \psi_i(x)|^2\, dx \geqslant 0, \tag{2.12}$$

Meecham determines the relationship involving the coefficients B_m for which the error ϵ is a minimum. It can be shown (see Appendix) that the desired relationship that satisfies the criterion is

$$\sum_{m=\min}^{\max} C_{nm} B_m = D_n \qquad (\min \leqslant n \leqslant \max) \tag{2.13}$$

where

$$C_{nm} = (1/a) \int_0^a \exp[+i2\pi(m-n)x/a]\, \psi_m(x)\, \psi_n^*(x)\, dx$$

$$D_n = (1/a) \int_0^a \exp[-i2\pi nx/a]\, \psi_i(x)\, \psi_n^*(x)\, dx. \tag{2.14}$$

Thus the problem has been reduced to solving simultaneously a finite set of equations for the coefficients B_m.

In our approach to the problem, we similarly define a new function $\chi_i(x)$ as was done in Eq. (2.11). Because the groove profile function $f(x)$ has period a, then so do the functions

$\psi_i(x)$, $\psi_m(x)$, and $\chi_i(x)$. This allows us to Fourier analyze these functions according to the equations

$$\left.\begin{aligned}
\psi_i(x) &= \sum_{j=-\infty}^{\infty} \psi_i^{(j)} \exp(-i2\pi jx/a) \\
\psi_m(x) &= \sum_{l=-\infty}^{\infty} \psi_m^{(l)} \exp(-i2\pi lx/a) \quad \text{(over all } m\text{)} \\
\chi_i(x) &= \sum_{j=-\infty}^{\infty} \chi_i^{(j)} \exp(-i2\pi jx/a).
\end{aligned}\right\} \tag{2.15}$$

If we now substitute the Fourier representation of $\psi_i(x)$, $\psi_m(x)$, and $\chi_i(x)$ as given by Eqs. (2.15) into Eqs. (2.9) and (2.11), we obtain

$$\left.\begin{aligned}
\sum_{j=-\infty}^{\infty} \psi_i^{(j)} \exp(-i2\pi jx/a) &= \sum_{m=-\infty}^{\infty} \sum_{l=-\infty}^{\infty} A_m \psi_m^{(l)} \exp[-i2\pi(l-m)x/a] \\
\sum_{j=-\infty}^{\infty} \chi_i^{(j)} \exp(-i2\pi jx/a) &= \sum_{m=\min}^{\max} \sum_{l=-\infty}^{\infty} B_m \psi_m^{(l)} \exp[-i2\pi(l-m)x/a].
\end{aligned}\right\} \tag{2.16}$$

By using the orthogonality property of the complex exponentials, it can be easily shown that

$$\left.\begin{aligned}
\psi_i^{(j)} &= \sum_{m=-\infty}^{\infty} A_m \psi_m^{(j+m)} \qquad \text{(over all } j\text{)} \\
\chi_i^{(j)} &= \sum_{m=\min}^{\max} B_m \psi_m^{(j+m)} \qquad \text{(over all } j\text{)}.
\end{aligned}\right\} \tag{2.17}$$

We now define a new error ϵ' according to the equation

$$\epsilon' = \sum_{j=-\infty}^{\infty} |\chi_i^{(j)} - \psi_i^{(j)}|^2 \geqslant 0. \tag{2.18}$$

We now want to find the relationship involving the coefficients B_m that minimizes the mean square error ϵ'. It can be shown that the desired relationship is given by

$$\sum_{m=\min}^{\max} C'_{nm} B_m = D'_n \qquad (\min \leqslant n \leqslant \max) \tag{2.19}$$

where now

$$\left.\begin{aligned} C'_{nm} &= \sum_{j=-\infty}^{\infty} \psi_m^{(j-m)}\, \psi_n^{(j-n)*} \\ D'_n &= \sum_{j=-\infty}^{\infty} \psi_i^{(j)}\, \psi_n^{(j-n)*}. \end{aligned}\right\} \tag{2.20}$$

Again the problem has been reduced to solving simultaneously a finite linear set of equations for the coefficients B_m. It turns out that the errors as defined by Eqs. (2.12) and (2.18) are in all respects equivalent. Thus our approach and that of Meecham are equivalent except for the fact that Meecham has done his analysis in the space domain whereas we have done our analysis in the Fourier frequency domain. We personally feel that our approach is more suitable for computer usage because of the time saving afforded by recent computer software for doing Fourier analysis.

2.1.2 Theory for the TM case

For the sake of completeness we present in this subsection the underlying theory for calculating diffraction efficiencies when the magnetic field vector of the incident beam is parallel to the grating grooves. The wave function associated with the incident field for this case is given by

$$\mathbf{H}_i(x,y,z,t) = [0,0,H_{iz}(x,y,z)]\, \exp(-i\omega t) \tag{2.21}$$

where the time-independent part of the wave function is given by

$$H_{iz}(x,y,z) = H_o \exp(-ikx \sin\theta_i) \exp(-iky \cos\theta_i). \tag{2.22}$$

Again k is the wavenumber, ω is the angular frequency, and θ_i is the angle of incidence.

By symmetry, the diffracted magnetic field vector will also be parallel to the z axis; that is,

$$\mathbf{H}_d(x,y,z,t) = [0,0,H_{dz}(x,y,z)]\, \exp(-i\omega t) \tag{2.23}$$

where now

$$H_{dz}(x,y,z) = -\sum_{m=-\infty}^{\infty} A_m \exp(+ikx \sin\theta_m) \exp(+iky \cos\theta_m). \tag{2.24}$$

The coefficients A_m are the unknown amplitude coefficients to be determined. The angles θ_m are again given by the grating equation.

The boundary condition that is to be satisfied at the grating surface for the TM case is that the normal derivative of the tangential component of the total magnetic field be identically equal to zero. Mathematically we have

$$\partial H_z(x,y,z)/\partial n_{|y=f(x)} = 0 \tag{2.25}$$

where

$$H_z(x,y,z) = H_{iz}(x,y,z) + H_{dz}(x,y,z). \tag{2.26}$$

It can be easily shown that the normal derivative operator is given by

$$\partial/\partial n = [1 + (f'(x))^2]^{-1/2}[-f'(x)(\partial/\partial x) + (\partial/\partial y)]. \tag{2.27}$$

Taking the normal derivative of Eqs. (2.22) and (2.24) and substituting the results into Eq. (2.25) gives

$$H_o\,(f'(x)\sin\theta_i - \cos\theta_i)\exp(-ikx\sin\theta_i)\exp(-ikf(x)\cos\theta_i)$$

$$= \sum_{m=-\infty}^{\infty} A_m\,(-f'(x)\sin\theta_m + \cos\theta_m)\,\exp(ikx\sin\theta_m)\exp(ikf(x)\cos\theta_m). \tag{2.28}$$

Without loss of generality we may conveniently let $H_o = -1$. With the use of the grating equation, Eq. (2.28) can be rewritten in the compact form

$$\psi_i(x) = \sum_{m=-\infty}^{\infty} A_m \exp(+i2\pi mx/a)\psi_m(x) \tag{2.29}$$

where the new functions $\psi_i(x)$ and $\psi_m(x)$ have been defined, again for purposes of convenience, by the equations

$$\left.\begin{aligned} \psi_i(x) &= (f'(x)\sin\theta_i - \cos\theta_i)\exp(-ikf(x)\cos\theta_i) \\ \psi_m(x) &= (f'(x)\sin\theta_m - \cos\theta_m)\exp(+ikf(x)\cos\theta_m)\,. \end{aligned}\right\} \tag{2.30}$$

On comparing Eqs. (2.29) and (2.9) we see that these equations have identical form. Therefore, the methods used in the last subsection for determining the unknown coefficients A_m can also be used in this subsection.

3. COMPUTER PROGRAM

The mathematical formulation of the diffraction grating problem is given in section 2. Based on this formulation a computer program was written to analyze such groove profiles as echelette, rectangular, sinusoidal, and cycloidal. Owing to the complexity of the mathematical calculations involved, the program was written in modular form; that is, the entire task was divided into a number of smaller subtasks. These subtasks constitute, for example, the generation of sampled values of the grating profile function, computation of the Fourier transform of various functions, and the inversion of matrices. Computer subroutines were written for each of the subtasks to be performed. Each subroutine was tested separately in proper sequence and then integrated together by the main program, which forms the logic center for the entire computer program. The main program consists mainly of call statements for calling the various subroutines to do their respective tasks.

The inputs to the computer program are

λ = wavelength
a = diffraction grating period
θ_i = angle of incidence
$f(x)$ = groove profile function
$f'(x)$ = groove slope function,

and the outputs are

θ_m = order m diffraction angle
B_m = order m amplitude coefficient
I_m = order m normalized intensity
ξ_m = order m diffraction efficiency.

Normalized intensities are quantities that can be experimentally measured. The normalized intensity associated with the m^{th} diffraction order is defined by the equation

$$I_m = |B_m|^2 / \sum_n |B_n|^2. \tag{3.1}$$

Only those amplitude coefficients B_m associated with the real or homogeneous diffraction orders are considered in the above definition.

To theoretically check on the accuracy of the computer calculation,[11] we can use the relationship

$$\sum_m |A_m|^2 (\cos\theta_m / \cos\theta_i) = 1, \tag{3.2}$$

which is derived from the conservation of energy law, where the term $|A_m|^2(\cos\theta_m/\cos\theta_i)$ represents the exact diffraction efficiency associated with the m^{th} diffraction order. The above sum is, again, restricted only to those orders that are real. The calculated diffraction efficiency for the m^{th} order is given by

$$\xi_m = |B_m|^2 (\cos\theta_m / \cos\theta_i). \tag{3.3}$$

The sum of the calculated diffraction efficiencies compared with unity serves as a check on the accuracy of the computer calculation.

After the computer program was written, a number of test cases were run to obtain results that could be directly compared with those already published in the literature (see subsection 3.1). Finally, we also studied the region of validity of our theory based on a total energy conservation check. Presented in subsection 3.2 are the results connected with the energy conservation check.

3.1 Test Cases

Several test cases were run and the results were compared with those published in the literature. Following is the comparison of results.

Test Case I: As a first check on the accuracy of the computer program, we compared the test results we obtained with those obtained by Meecham and Peters[1,2] for the E-parallel state of polarization. The groove profile considered was an echelette type as shown in Fig. 3.1. The inputs were

λ = 1.33 inches (microwave wavelength)
a = 1.75 inches
θ_i = variable
ψ = 90.0°
α = 8.2°.

The outputs were the normalized intensity values I_m. The comparison of results is shown in Fig. 3.2. Also included are experimental results that Meecham and Peters[1,2] published as a comparison between theory and experiment.

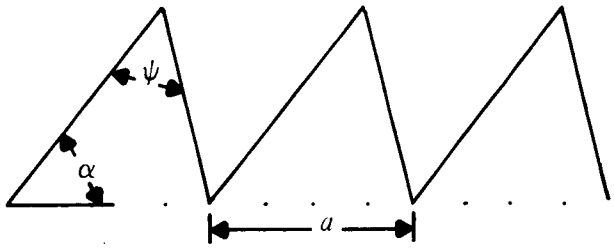

Fig. 3.1. Echelette grating profile.

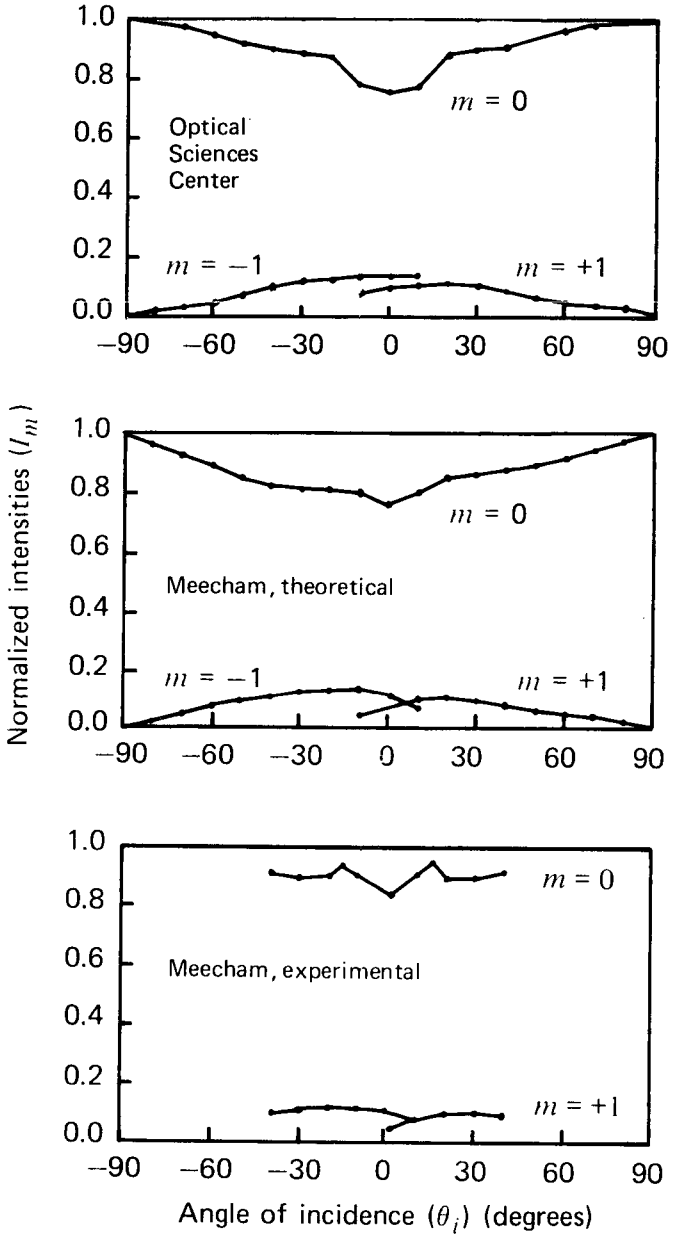

Fig. 3.2. Comparison of test results of the Optical Sciences Center with the theoretical and experimental results of Meecham.

Test Case II: As a second check on the computer program, we compared test results we obtained with those predicted by the integral equation approaches of Kalhor and Neureuther[8] and Petit.[13] The grating profile considered was again an echelette type, Fig. 3.1. For this case the inputs to the computer program were

λ = 0.546 μm (optical wavelength)
a = 1.250 μm
θ_i = 0.0°
ψ = 162.9°, 146.6°, 90.0°
α = 8.5°, 16.7°, 45.0°.

The outputs were the normalized intensity values I_m. The comparison of results is tabulated in Tables 3.1 and 3.2. Table 3.1 corresponds to the E-parallel state, and Table 3.2 corresponds to the H-parallel state of polarization. Also included for comparison are the total diffraction efficiencies associated with each of the calculations. Due to the symmetry involved in this case, the normalized intensity of the $-m^{th}$ order is identical to the normalized intensity of the $+m^{th}$ order. Therefore, only normalized intensity values associated with the positive orders have been tabulated.

Table 3.1 Normalized intensity coefficients for the E-parallel case.

Grating	Investigator	I_0	I_1	I_2	Total efficiency
ψ=162.9, α=8.5	Kalhor	0.671	0.156	0.008	1.000
	Petit	0.671	0.157	0.008	0.999
	Optical Sciences	0.667	0.159	0.008	1.000
ψ=146.6, α=16.7	Kalhor	0.153	0.335	0.089	0.999
	Petit	0.151	0.334	0.090	0.999
	Optical Sciences	0.152	0.335	0.089	0.998
ψ=90.0, α=45.0	Kalhor	0.347	0.081	0.246	0.995
	Petit	0.333	0.083	0.250	1.034
	Optical Sciences	0.280	0.100	0.260	0.672

Table 3.2 Normalized intensity coefficients for the H-parallel case.

Grating	Investigator	I_0	I_1	I_2	Total efficiency
ψ=162.9, α=8.5	Kalhor	0.609	0.174	0.022	1.001
	Petit	0.617	0.177	0.014	0.997
	Optical Sciences	0.606	0.173	0.024	1.000
ψ=146.6, α=16.7	Kalhor	0.098	0.247	0.204	0.977
	Petit	0.098	0.243	0.208	0.994
	Optical Sciences	0.099	0.244	0.206	0.996
ψ=90.0, α=45.0	Kalhor	0.689	0.043	0.113	1.006
	Petit	Results not available			
	Optical Sciences	0.535	0.014	0.218	0.452

Test Case III: As a third check on the computer program, we compared the test results we obtained with those predicted by Maystre and Petit.[7] The grating profile considered was that of a cycloid as depicted in Fig. 3.3. The cycloid profile has been used as an approximation to one type of holographic grating profile and is described mathematically by the set of parametric equations

$$f(x) = B + B\cos(2\pi u/a)$$
$$x = u + A\sin(2\pi u/a) \tag{3.4}$$

where u is the parameter. The inputs to the program were

$\lambda = 0.450\ \mu m$ (optical wavelength)
$a = 0.769\ \mu m$
$\theta_i = -10.5°$
$A = 0.069\ \mu m$
$B = 0.092, 0.138, 0.185, 0.231\ \mu m.$

Only the E-parallel state of polarization was considered for this test case. The output was the diffraction efficiency for the -1^{st} order. Table 3.3 contains the comparison of the results.

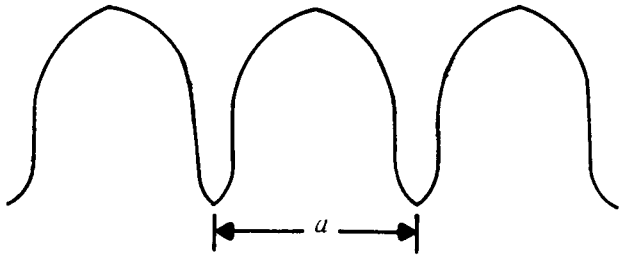

Fig. 3.3. Cycloidal grating profile.

Table 3.3. -1^{st} order diffraction efficiency for the E-parallel case.

Grating	Investigator	ξ_{-1}
A = 0.069	Petit	0.212
B = 0.092	Optical Sciences	0.233
A = 0.069	Petit	0.425
B = 0.138	Optical Sciences	0.416
A = 0.069	Petit	0.525
B = 0.185	Optical Sciences	0.553
A = 0.069	Petit	0.675
B = 0.231	Optical Sciences	0.612

Test Case IV: As a final check on the program we again compared our test results with those published by Maystre and Petit.[7] The cycloid grating profile was the profile of interest. The inputs were

λ = 0.450 μm (optical wavelength)
a = 0.769 μm
θ_i = variable
A = 0.069 μm
B = 0.092 μm.

The output to the computer programs was the diffraction efficiency of the -1^{st} order. Figure 3.4 shows the efficiency of the -1^{st} order for various angles of incidence for the E-parallel state of polarization. Similarly, Fig. 3.5 shows the results for the H-parallel state of polarization.

3.2 Energy Conservation Check

In order to further evaluate the region of validity of the E-parallel and H-parallel calculations, we investigated the influence that groove depth has on the accuracy of the computer calculations. This investigation is important because in any correct calculation the total diffraction efficiency must be equal to unity. The departure of total efficiency from unity serves to indicate where the calculation ceases to be useful. For this investigation we chose a symmetrical echelette grating profile for the analysis. Eight test cases were run. The distinction between these test cases is summarized in Table 3.4. There were two independent variables of interest. The first was the groove-depth-to-wavelength ratio and the second was the groove-depth-to-grating-period ratio. The latter ratio is proportional to the absolute slope of the grating facets for the symmetrical echelette case. The dependent variable of interest is the total diffraction efficiency. Again the total diffraction efficiency serves as an energy conservation check. For total efficiency values near unity we consider the predicted values of the individual diffraction order efficiencies to be reliable. Total efficiency values differing greatly from unity indicate where the underlying theory is breaking down. Summarized in Figs. 3.6 through 3.9 are the results of these eight test cases. The total efficiency has been plotted against both the groove-depth-to-wavelength ratio and the groove-depth-to-grating-period ratio.

Table 3.4 Analysis of symmetrical echelette grating for eight test cases.

Test case	Polarization state	Grating constant	Wavelength	Incidence angle (deg)	Absolute slope
I	E-parallel	1.4	1.0	0.0	0.0 to 1.0
II	H-parallel	1.4	1.0	0.0	0.0 to 1.0
III	E-parallel	5.0	1.0	0.0	0.0 to 1.0
IV	H-parallel	5.0	1.0	0.0	0.0 to 1.0
V	E-parallel	1.4	1.0	−80.0	0.0 to 1.0
VI	H-parallel	1.4	1.0	−80.0	0.0 to 1.0
VII	E-parallel	5.0	1.0	−80.0	0.0 to 1.0
VIII	H-parallel	5.0	1.0	−80.0	0.0 to 1.0

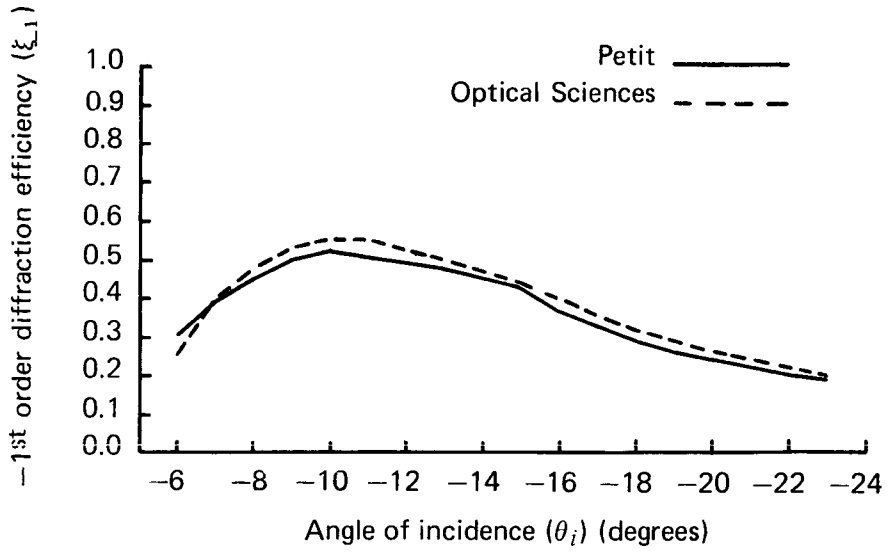

Fig. 3.4. Efficiency of the -1^{st} order for various angles of incidence for the E-parallel state of polarization.

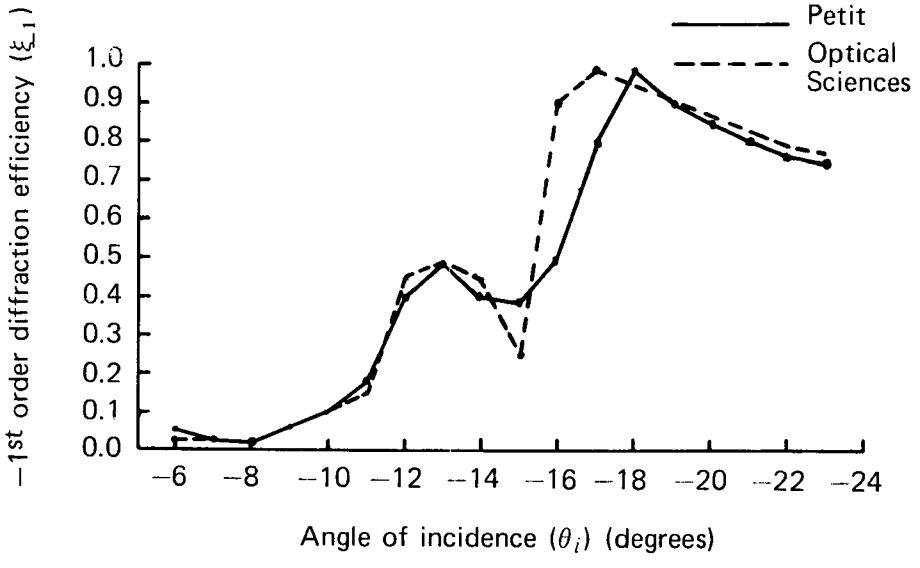

Fig. 3.5. Efficiency of the -1^{st} order for various angles of incidence for the H-parallel state of polarization.

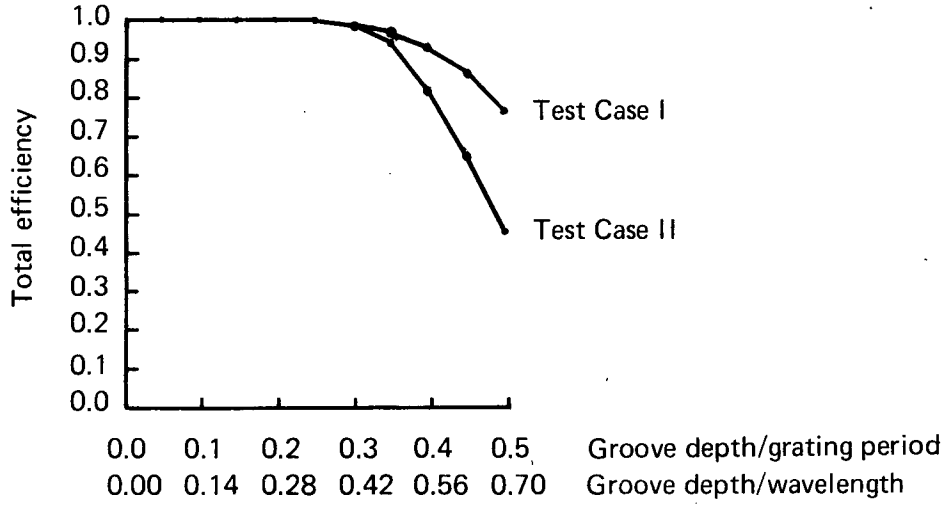

Fig. 3.6 Total efficiency as a function of groove-depth-to-grating-period ratio and groove-depth-to-wavelength ratio for test cases I and II.

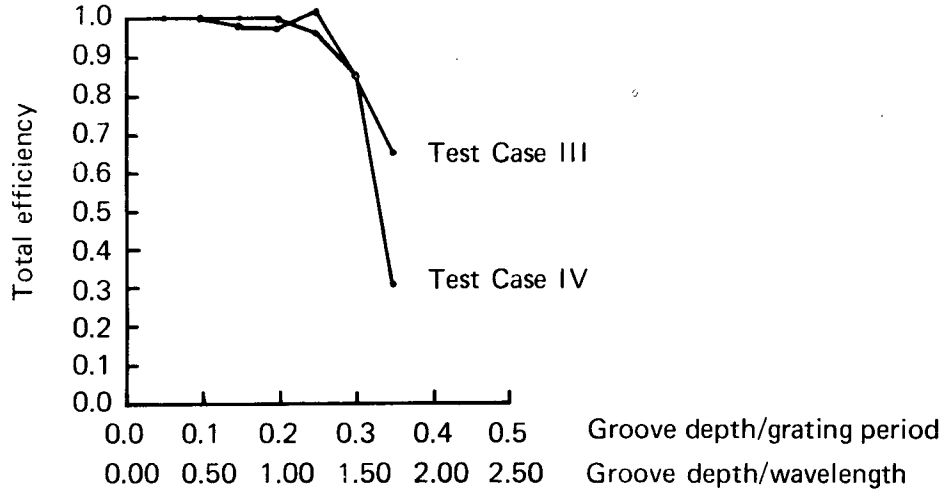

Fig. 3.7. Total efficiency as a function of groove-depth-to-grating-period ratio and groove-depth-to-wavelength ratio for test cases III and IV.

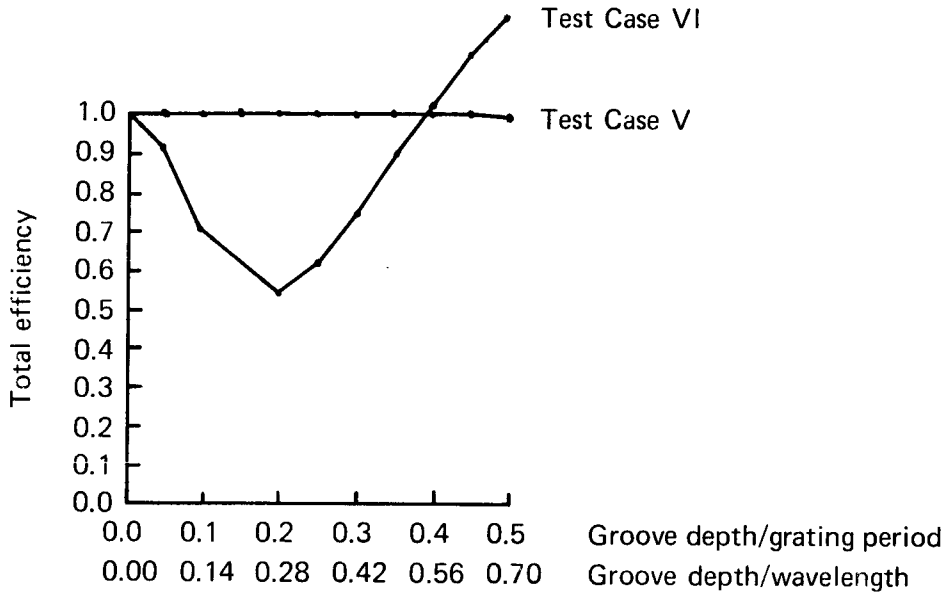

Fig. 3.8. Total efficiency as a function of groove-depth-to-grating-period ratio and groove-depth-to-wavelength ratio for test cases V and VI.

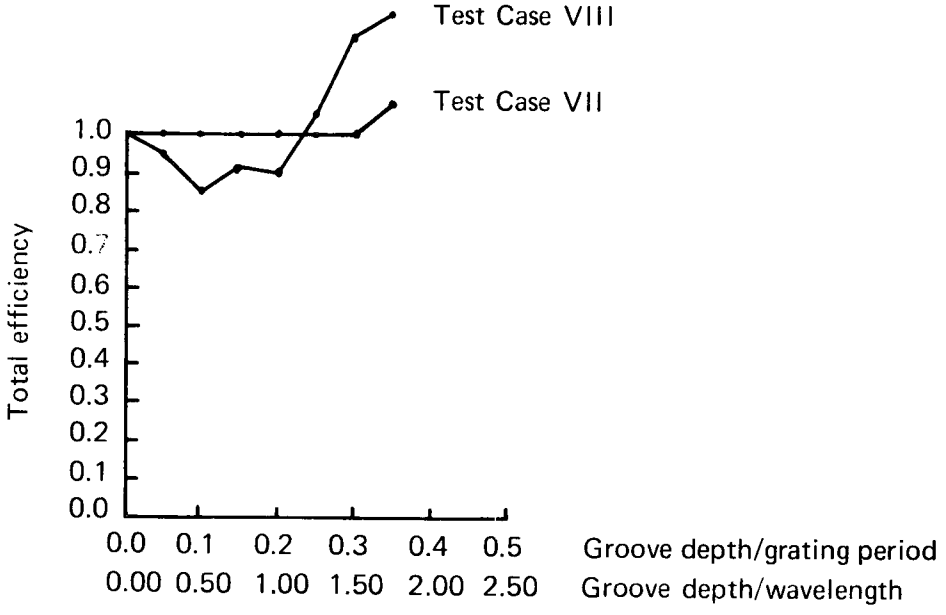

Fig. 3.9. Total efficiency as a function of groove-depth-to-grating-period ratio and groove-depth-to-wavelength ratio for test cases VII and VIII.

3.3 Conclusions

The agreement between our results and those published in the literature are, in general, rather good. There is one case, namely the symmetrical echelette ($\alpha = 45°, \psi = 90°$), where the agreement is poor although a similar trend is definitely apparent. Again, the basis of our computer program is the assumption that the diffracted field can be represented as a superposition of plane waves with constant amplitude coefficients. As is discussed in the dissertation by Kalhor,[11] this assumption is not valid for diffracted fields within the groove region; that is, the plane wave amplitude coefficients depend upon spatial position within the groove region. But this assumption is rather good for shallow groove gratings as is evident from the results.

The results of the energy conservation check give us an idea about the region of validity of the plane wave theory with constant coefficients. For normal incidence, the plane wave theory breaks down for groove-depth-to-grating-period ratios greater than about 0.25 for both the E-parallel and H-parallel polarization states. For grazing incidence, the E-parallel case does quite well for groove-depth-to-grating-period ratios as large as 0.5. The H-parallel case breaks down immediately for the case of grazing incidence. Thus the plane wave theory has a smaller region of validity for the H-parallel polarization state than for the E-parallel polarization state. But within the region of validity, the plane wave theory is as acceptable as the integral-equation approaches of either Kalhor or Petit.

4. POLARIZING GRATINGS

One of the goals of interest in diffraction grating analysis is to design a diffraction grating that will polarize the light in a prespecified diffraction order for any arbitrary state and/or degree of incident polarized light.

4.1 Discussion

The profile chosen for this investigation was that of an echelette as shown in Fig. 4.1. A geometrical argument was used to determine the initial values of the angle of incidence, wavelength, and grating period in terms of the base angle α for the case when light would be completely polarized in a prespecified order.

Fig. 4.1. Echelette grating profile.

We chose the apex angle ψ to equal 90° and the angle of incidence θ_i to equal $-\alpha$. We then considered the case when the magnetic field vector of the incident wave is parallel to the grooves of the grating. The incident electromagnetic field interacts with the diffraction grating in such a manner that each elemental unit of charge induced on the surface of the grating effectively behaves as a dipole radiator. The axes of these dipole radiators lie in the plane orthogonal to the grating grooves and point in the direction $90° - \alpha$. If we now choose one of the diffraction angles to be equal to $90° - \alpha$, then little or no energy should be radiated into the corresponding order for this state of polarization because dipole radiators do not radiate along their axes.

To test the geometrical argument, consider the following example. Let the diffraction order of interest be the $+1^{st}$ order. According to the geometrical argument, we have

$$\begin{aligned} \theta_i &= -\alpha \\ \theta_1 &= 90° - \alpha. \end{aligned} \tag{4.1}$$

Using the grating equation yields the result

$$\lambda/a = \cos\alpha - \sin\alpha. \tag{4.2}$$

Thus if we choose the base angle α, the wavelength λ, and the grating period a to satisfy Eq. (4.2), then, according to the geometrical argument, the diffraction grating should behave as

a linear polarizer in the $+1^{st}$ diffraction order. For example, when unpolarized light is incident, it may be decomposed into a component lying entirely in the plane of incidence and another component perpendicular to the plane of incidence. The component in the plane of incidence (H-parallel) will yield no contribution in the $+1^{st}$ order. When a similar reasoning is followed for the component perpendicular to the plane of incidence (E-parallel), it may be easily shown that it will in general yield a nonzero contribution of energy in the $+1^{st}$ order. The energy distribution of this order for this polarization is not predicted by the geometrical argument. It can only be predicted by a wave theoretic calculation.

We now turn our attention to a specific computer calculation based on the preceding discussion. Suppose we wish to design an echelette profile diffraction grating so that no energy appears in the $+1^{st}$ order for the H-parallel state of polarization at a wavelength of 0.5 μm. Suppose we also arbitrarily choose the grating period to be equal to 0.6375 μm. Then according to Eq. (4.2) we should choose $\alpha = 11.3°$. Thus the initial inputs to the computer program are

$\theta_i = -11.3°$
λ = variable
$a = 0.6375\ \mu$m
$\alpha = +11.3°$
$\psi = +90.0°$.

Summarized in Figs. 4.2 and 4.3 are the results of this calculation. Plotted in these figures are the normalized intensity values for the real orders versus the wavelength λ. Figure 4.2 corresponds to the E-parallel case, and Fig. 4.3 corresponds to the H-parallel case. We see from Fig. 4.2 that the normalized intensity associated with the $+1^{st}$ order has a fairly constant value for those wavelengths indicated. From Fig. 4.3 we see that the normalized intensity associated with the $+1^{st}$ order goes to zero but at a shorter wavelength than predicted by the geometrical argument.

4.2 Conclusions

The geometrical argument presented in subsection 4.1 has allowed us to predict, before making any computer calculations, the wavelength and diffraction order in which the diffracted light would be completely linearly polarized. By working in the neighborhood of this wavelength, we showed that the intensity of the $+1^{st}$ order for the H-parallel case does indeed go to zero but at a shorter wavelength than geometrically predicted.

A similar shift in wavelength has been reported by Kalhor.[11] For a given echelette grating, Kalhor predicted with a geometrical argument the wavelength, angle of incidence, and diffraction order at which maximum blazing should occur. He tested his prediction with a computer program based on a rigorous electromagnetic theory. By working in the neighborhood of the predicted wavelength, he showed that maximum blazing actually occurs but at a smaller wavelength. Thus we have another example of a model based on only geometrical considerations that was used to give insights about a phenomenon. Therefore, the use of such a tool in grating design does indeed have significant importance.

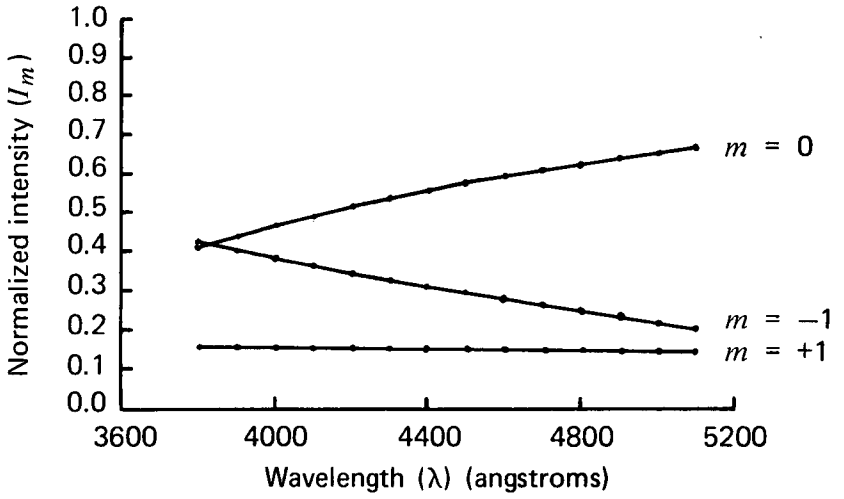

Fig. 4.2. Normalized intensity values for the real orders vs wavelength for the E-parallel state of polarization. The angle of incidence is −11.3° and the grating period is 0.6375 μm.

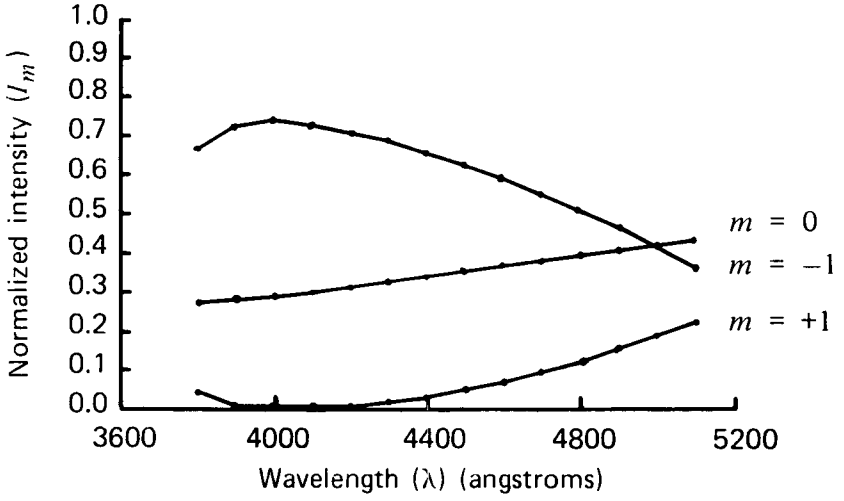

Fig. 4.3. Normalized intensity values for the real orders vs wavelength for the H-parallel state of polarization. The angle of incidence is −11.3° and the grating period is 0.6375 μm.

5. BLAZED GRATINGS

One of the most important uses of diffraction gratings is for the spectroscopic study of light emitted from various types of light sources. The spectrum is usually observed in one diffraction order only, and light that is diffracted into the other orders may be considered to be wasted. Therefore, in spectroscopic applications, it is desirable to concentrate as much of the incident light energy into a single dispersive diffraction order. Gratings that have this property are referred to as blazed diffraction gratings. In contrast, unblazed gratings allow a large fraction of the incident light energy to reappear in the nondispersive zero diffraction order. In this section we will be concerned with the design of blazed diffraction gratings.

5.1 Discussion

In the design of blazed diffraction gratings we first determine the wavelength for which the grating is to be blazed. We then choose values of the grating constant and the angle of incidence so that there are only two real diffraction orders, namely the nondispersive zero order and the dispersive -1^{st} order. We thereby reduce the number of real orders competing for the energy initially contained in the incident beam of light. Next the groove profile parameters, the angle of incidence, and the grating period are varied to optimize the case when a large fraction of the incident light energy is diffracted into the -1^{st} order.

Two echelette grating profiles were considered in the blazed grating analysis: a mechanically ruled 90° echelette and an echelette with rounded edges (see Fig. 5.1). Sheridon[14] reports that diffraction gratings with rounded edges have been made from photoresist materials by means of the holographic process.

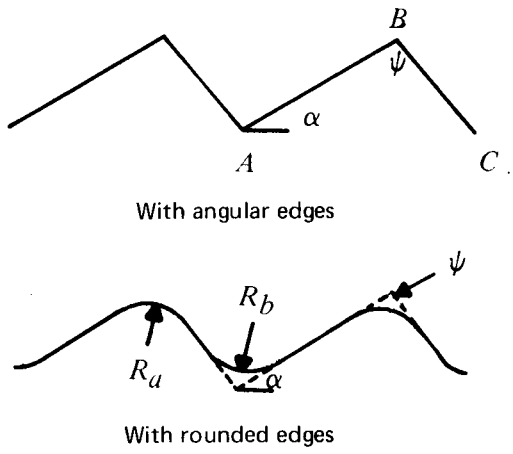

Fig. 5.1. Two echelette grating profiles that were considered in the blazed grating analysis.

5.1.1 Echelette grating profile

The grating profile we initially chose to analyze was the echelette type. A geometrical argument was used to pick the initial values of the angle of incidence and the grating constant to begin the computer analysis. For echelette diffraction gratings, the geometrical argument says that blazing of order m occurs when the rays reflected from one of the grating facets of the grooves have the same direction as the grating order m. For our analysis the diffraction order of interest is the -1^{st} order.

Referring to Fig. 5.1, we choose the angle of incidence at which an incident ray strikes the facet AB at a normal. Therefore, the angle of incidence is initially given by

$$\theta_i = -\alpha. \tag{5.1}$$

According to the geometrical argument the incident rays will be reflected back into the direction from which they came. Therefore, we choose the direction of the -1^{st} order according to

$$\theta_{-1} = -\alpha. \tag{5.2}$$

Substituting Eqs. (5.1) and (5.2) into the grating equation for $m = -1$ yields

$$\lambda/a = 2\sin\alpha. \tag{5.3}$$

In order to guarantee that the -1^{st} order and the zero order are the only two real diffraction orders, we must be sure that the inequality

$$\lambda/a \geqslant 2/3 \tag{5.4}$$

is satisfied when Eq. (5.3) is used. For wavelength-to-grating-period ratios less than 2/3 it can be easily shown that at least three diffraction orders will be real. If we arbitrarily choose the base angle α to be equal to 30°, then from Eq. (5.3) we find

$$\lambda/a = 1.000, \tag{5.5}$$

which satisfies inequality (5.4). Thus, for a base angle of 30°, the geometrical argument predicts that maximum blazing will occur in the -1^{st} order if the grating period is chosen to be equal to the wavelength of interest.

Next we must test the validity of the geometrical argument by using the computer to calculate the energy distribution in the -1^{st} order. The necessary inputs to the computer program for this test are

$\alpha = 30°$
$\psi = 90°$
$\theta_i = -30°$
λ/a = variable.

The computer analysis was restricted to the E-parallel state of polarization only. The calculation was attempted for the H-parallel case, but the results were rejected because of a large departure of the total efficiency from unity. The results of this initial calculation are shown in Fig. 5.2, where we plot the normalized intensity for the -1^{st} order versus the ratio (λ/a). We see that a large fraction of the total energy is indeed contained in the -1^{st} order but that the curve is a maximum at the ratio 0.786 and not at the geometrically predicted ratio of 1.000. The value of the normalized intensity for the -1^{st} order at the ratio 0.786 for this calculation is equal to 0.88, a fairly large value.

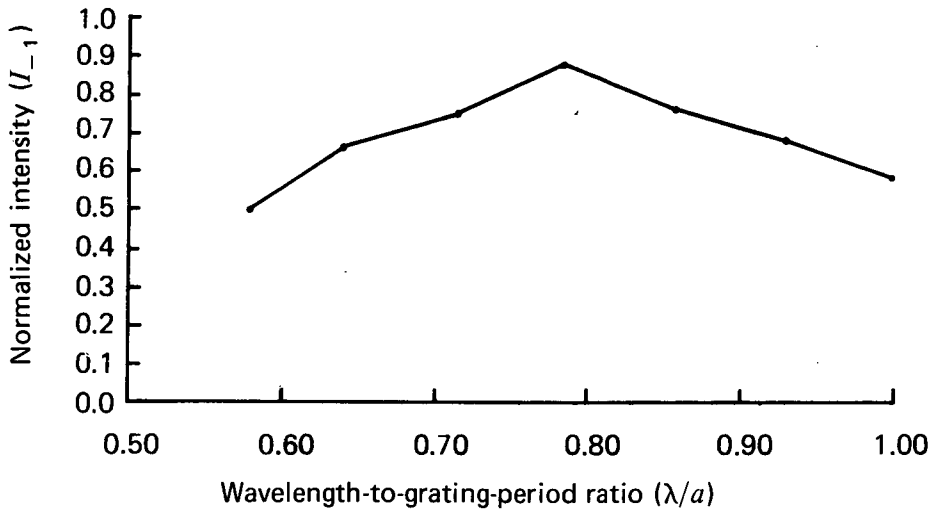

Fig. 5.2. Normalized intensity for the -1^{st} order vs the ratio (λ/a) for the E-parallel state of polarization. The angle of incidence is $-30°$.

Kalhor[11] reported similar results obtained for an echelette grating with base angles of 25.5° and 64.5°. He showed that the intensity associated with the -1^{st} order was a maximum at a shorter wavelength than that predicted by the geometrical argument. He did not optimize his solution by varying other parameters. Based on the calculations he did make, he concluded that about 90% of the incident energy could be diffracted into the -1^{st} order. He considered the E-parallel state of polarization only.

We continued with our analysis in order to further optimize the solution. We chose the wavelength-to-grating-period ratio to be 0.786 and varied the angle of incidence to see if angles of incidence other than $-30.0°$ might give higher values of the normalized intensity for the -1^{st} order. We found in fact that $-19.0°$ was a more desirable angle of incidence to use. Next we chose the angle of incidence to be $-19.0°$ and varied the wavelength-to-grating-period ratio to see if still further improvement could be made. Continuing in this manner allowed us to converge upon a solution for which 99% of the incident light energy reappeared in the -1^{st} order. The angle of incidence and the wavelength-to-grating-period ratio for which this maximum blazing occurred were found to be

$$\theta_i = -19.47122°$$
$$\lambda/a = 0.66667.$$

Figure 5.3 is a plot of the normalized intensity versus the wavelength-to-grating-period ratio for the -1^{st} order for the E-parallel state of polarization. The ratio 2/3 and the angle of incidence $-19.47122°$ define a double Wood's anomaly condition for the $+1^{st}$ and -2^{nd} diffraction orders. That is, when the wavelength-to-grating-period ratio is equal to 2/3 and the angle of incidence is equal to $-19.47122°$, we find that both the $+1^{st}$ and -2^{nd} diffraction orders are simultaneously changing from evanescent to real diffraction orders. This can be seen by using the grating equation for $m = +1$ and $m = -2$ with $\theta_{+1} = +90.0°$ and $\theta_{-2} = -90.0°$. That is,

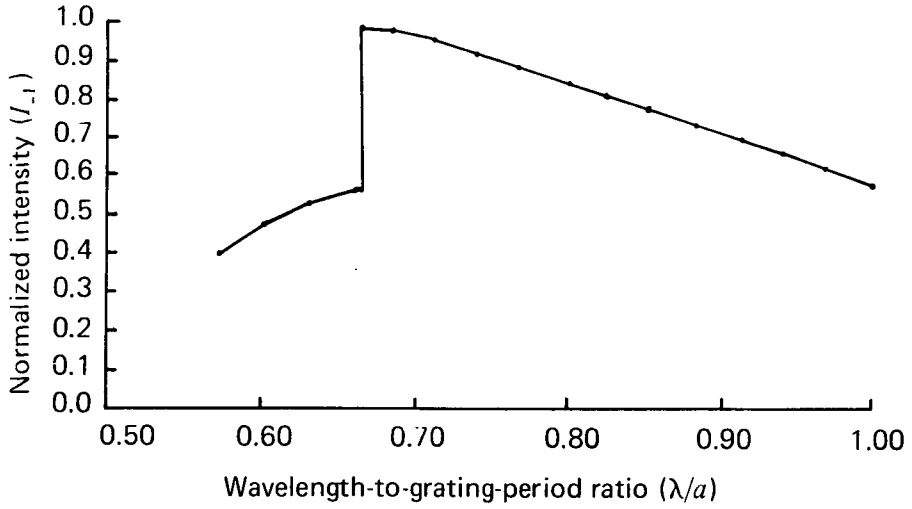

Fig. 5.3. Normalized intensity for the -1^{st} order vs the ratio (λ/a) for the E-parallel state of polarization. The angle of incidence is $-19.47122°$.

$$\sin(+90.0°) + \sin\theta_i = +1(\lambda/a) \tag{5.6a}$$
$$\sin(-90.0°) + \sin\theta_i = -2(\lambda/a) \tag{5.6b}$$

or equivalently

$$+1.0 + \sin\theta_i = +1(\lambda/a) \tag{5.7a}$$
$$-1.0 + \sin\theta_i = -2(\lambda/a). \tag{5.7b}$$

Adding Eqs. (5.7a) and (5.7b) yields

$$\lambda/a = -2\sin\theta_i. \tag{5.8}$$

Equation (5.8) is the Bragg equation, which has been used by Hessel and Shmoys[15] in the design of blazed diffraction gratings with rectangular profiles. If we subtract Eq. (5.7a) from Eq. (5.7b), we find

$$\lambda/a = 2/3. \tag{5.9}$$

Substituting this ratio back into Eq. (5.7a) gives

$$\sin\theta_i = -1/3, \tag{5.10}$$

which yields

$$\theta_i = \sin^{-1}(-1/3) = -19.47122°. \tag{5.11}$$

Thus we have established that an echelette grating exhibits excellent blazing properties in the region of the double Wood's anomaly associated with the $+1^{st}$ and -2^{nd} diffraction orders for the E-parallel state of polarization. This result we propose to publish in the *Journal of the Optical Society of America.*

5.1.2 Echelette grating profile with rounded edges

The second grating profile that we investigated, in terms of its blazing properties, was that of an echelette with rounded edges. As was previously indicated, gratings with this type of profile have been made from photoresist material using the holographic process. This profile is depicted in Fig. 5.1. Four quantities are needed to specify the rounded echelette profile. These quantities are the angles α and ψ and the radii R_a and R_b. We note that when R_a and R_b are zero a perfect echelette with no rounded edges results. It was shown in the previous section that an echelette grating with a base angle of 30.0° and an apex angle of 90.0° exhibits excellent blaze properties in the neighborhood of a double Wood's anomaly for the E-parallel state of polarization. We were interested to see what effect rounding the edges would have on the blaze properties of an echelette grating. Thus we ran similar test cases as was done in the previous section. The inputs to the computer program were

$\theta_i = -19.47122°$
$\alpha = 30.0°$
$\psi = 90.0°$
λ/a = variable
$R_a/a = 0.07, 0.14, 0.21$
$R_b/a = 0.07, 0.14, 0.21.$

The results of this calculation are summarized in Figs. 5.4, 5.5, and 5.6. In each of these figures is plotted the normalized intensity for the -1^{st} order versus the wavelength-to-grating-period ratio for the E-parallel state of polarization. First let us look at Fig. 5.4, which corresponds to the case when $R_a/a = R_b/a = 0.07$. Comparing the plot in this figure with the plot in Fig. 5.3 for the perfect echelette, we see that the plots are nearly identical. Again the curve is a maximum at a wavelength-to-grating-period ratio of 2/3 with a value of 0.985. Figure 5.5 corresponds to the case when $R_a/a = R_b/a = 0.14$. The maximum value of the curve has dropped to 0.970. The results for the worst rounded case are presented in Fig. 5.6. Referring to this figure we see that the curve has a maximum value of 0.910, a rather large value. It is noted that an echelette grating with $\alpha = 30°$, $\psi = 90°$, and $R_a/a = R_b/a = 0.21$ has only 50% of the flat facet area of a perfect echelette with no rounding. Also this rounded echelette is the shallowest of the gratings analyzed. For this reason the worst rounded echelette could be analyzed for the H-parallel state of polarization. The results are presented in Fig. 5.7. We see from this figure that the rounded echelette has excellent blaze properties over a large wavelength region.

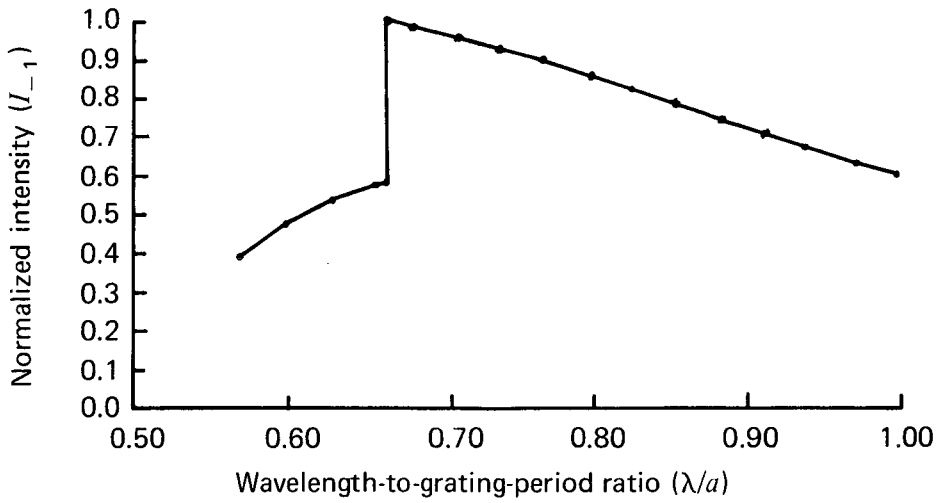

Fig. 5.4. Normalized intensity vs wavelength-to-grating-period ratio (λ/a) for the E-parallel state of polarization. The angle of incidence is $-19.47122°$ and $R_a/a = 0.07$, $R_b/a = 0.07$.

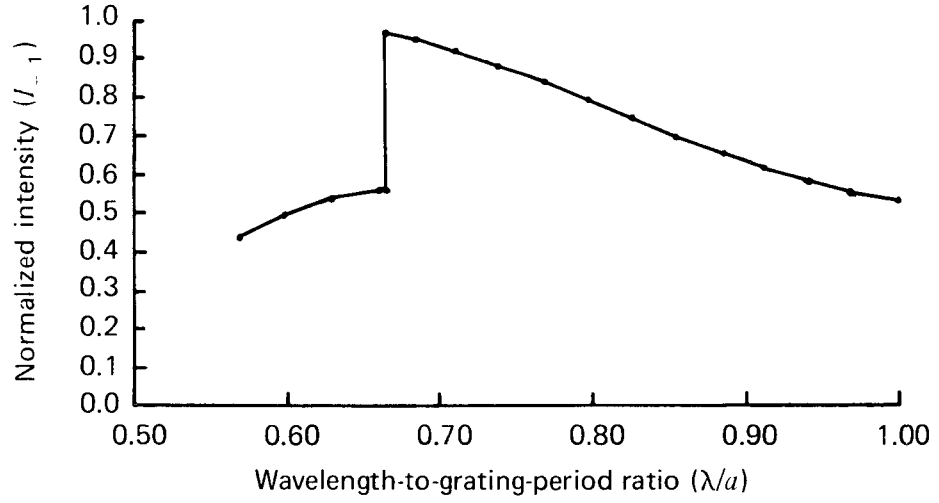

Fig. 5.5. Normalized intensity vs wavelength-to-grating-period ratio (λ/a) for the E-parallel state of polarization. The angle of incidence is $-19.47122°$ and $R_a/a = 0.14$, $R_b/a = 0.14$.

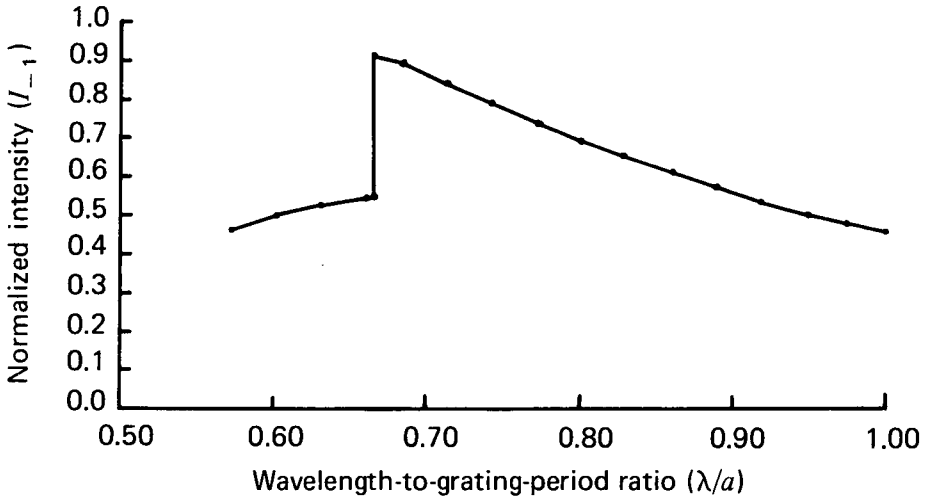

Fig. 5.6. Normalized intensity vs wavelength-to-grating-period ratio (λ/a) for the E-parallel state of polarization. The angle of incidence is $-19.47122°$ and $R_a/a = 0.21$, $R_b/a = 0.21$.

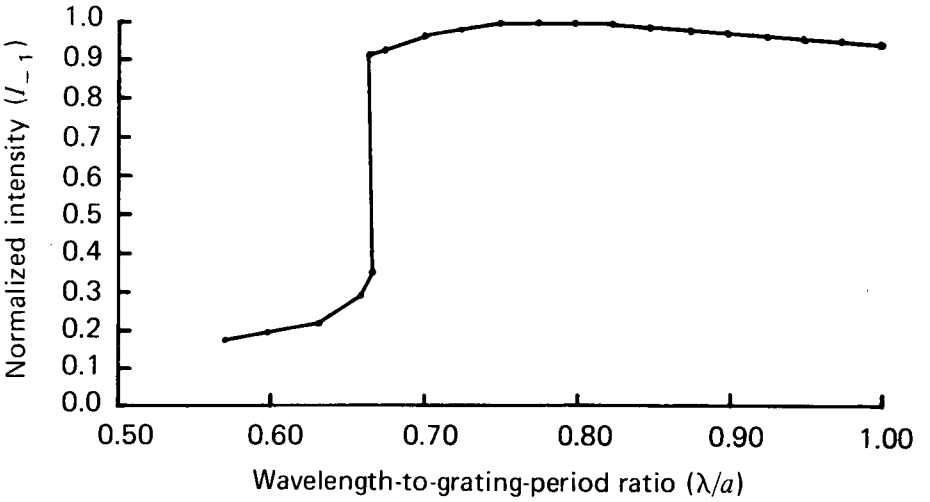

Fig. 5.7. Normalized intensity vs wavelength-to-grating-period ratio (λ/a) for the H-parallel state of polarization. The angle of incidence is $-19.47122°$ and $R_a/a = 0.21$, $R_b/a = 0.21$.

5.2 Conclusions

The following conclusions were drawn based on the results of the analysis done in this section.

A. Geometrical arguments are very useful in the preliminary design stages of blazed diffraction gratings. These arguments are used to choose initial values of the various grating parameters needed to begin the computer analysis. These parameters are then varied inside of the computer in order to find the optimum solution.

B. Echelette profiles with and without rounded edges exhibit excellent blaze properties in the vicinity of the double Wood's anomaly associated with the $+1^{st}$ and the -2^{nd} diffraction orders. The conditions necessary for the existence of this double Wood's anomaly are

$$\theta_i = \sin^{-1}(-1/3) = -19.47122^\circ$$
$$\lambda/a = 2/3 = 0.66667.$$

For a perfect echelette profile it was shown that on the order of 99% of the energy in the incident wave reappeared in the dispersive -1^{st} order for the E-parallel state of polarization in the anomalous region. For the echelette profile with the worst rounding it was shown that on the order of 91% of the energy in the incident beam reappeared in the -1^{st} order for both the E- and H-parallel states of polarization. Thus, echelette gratings with rounded edges, which can be made holographically, do indeed exhibit excellent blaze properties.

APPENDIX

MEAN SQUARE ERROR MINIMIZATION

In this appendix we outline how to obtain Eq. (2.13) of the text, namely

$$\sum_{m=\min}^{\max} C_{nm} B_m = D_n \qquad (\min \leqslant n \leqslant \max).$$

This relationship determines B_m so that the error ϵ as defined in Eq. (2.12), namely

$$\epsilon = (1/a) \int_0^a |\chi_i(x) - \psi_i(x)|^2 dx \geqslant 0,$$

is minimized.

We propose to minimize the mean square error ϵ by differentiating ϵ with respect to B_m^* and setting the result equal to zero. B_m^* is the complex conjugate of B_m. The coefficients B_m are part of the definition of the function $\chi_i(x)$, Eq. (2.11). This differentiation does not affect the coefficients B_m of $\chi_i(x)$ because B_m and B_m^* are linearly independent.

Substituting the complex conjugate of Eq. (2.11) into Eq. (2.12) and rearranging gives

$$\epsilon = \sum_{m=\min}^{\max} B_m^* (1/a) \int_0^a \chi_i(x) \psi_m^*(x) \exp(-i2\pi mx/a) dx$$

$$- \sum_{m=\min}^{\max} B_m^* (1/a) \int_0^a \psi_i(x) \psi_m^*(x) \exp(-i2\pi mx/a) dx$$

$$+ (1/a) \int_0^a \psi_i(x) \psi_i^*(x) dx$$

$$- (1/a) \int_0^a \chi_i(x) \psi_i^*(x) dx. \tag{A1}$$

The total differential of ϵ is

$$d\epsilon = \sum_{n=\min}^{\max} (\partial \epsilon / \partial B_n^*) dB_n^*. \tag{A2}$$

Because we are interested in minimizing ϵ, then we see that $d\epsilon$ is equal to zero, which implies

$$\partial\epsilon/\partial B_n^* = 0 \qquad (\min \leqslant n \leqslant \max).$$

Thus, differentiating ϵ of Eq. (A1) with respect to B_n^* and setting the result equal to zero yields

$$(1/a)\int_0^a \chi_i(x)\psi_n^*(x)\exp(-i2\pi nx/a)dx$$

$$= (1/a)\int_0^a \psi_i(x)\psi_n^*(x)\exp(-i2\pi nx/a)dx. \tag{A3}$$

In the above expression on the left side we substitute the expression for $\chi_i(x)$ from Eq. (2.11) in the text. We obtain

$$\sum_{m=\min}^{\max} C_{nm}B_m = D_n \qquad (\min \leqslant n \leqslant \max) \tag{A4}$$

where we defined

$$C_{nm} = (1/a)\int_0^a \exp[-i2\pi(n-m)x/a]\,\psi_n^*(x)\psi_m(x)dx$$

$$D_n = (1/a)\int_0^a \exp[-i2\pi nx/a]\,\psi_n^*(x)\psi_i(x)dx.$$

Equation (A4) is the desired result.

REFERENCES

[1] Antonie Labeyrie, "Holo-gratings – the new diffraction breed," Electro-Optical Systems Design, pp. 32-38, February 1971.

[2] E. G. Loewen, "Modern diffraction gratings," Electro-Optical Systems Design, pp. 20-27, October, 1970.

[3] R. F. Stamm and J. J. Whalen, "Energy distribution of diffraction gratings as a function of groove form," J. Opt. Soc. Am. 36(1):2-12, 1946.

[4] Masao Seya and Katsuya Goto, "On the energy distributions of diffracted light from plane gratings," Science of Light 5(3):119-129, 1956.

[5] G. W. Stroke, "Diffraction gratings," in *Handbuch des Physik,* Vol. 29, S. Flugge, ed., Berlin, Springer-Verlag, 1967.

[6] James Pavageau and Jacqueline Bousquet, "Diffraction par un réseau conducteur nouvelle méthode de résolution," Optica Acta 17(6):469-470, 1970.

[7] D. Maystre and R. Petit, "Sur la détermination du champ diffracté par un réseau holographique," Optics Communications 2(7):309-311, 1970.

[8] H. A. Kalhor and A. R. Neureuther, "Numerical method for the analysis of diffraction gratings," J. Opt. Soc. Am. 61(1):43-48, 1971.

[9] M. Neviere, G. Cerutti-Maori, and M. Cadilhac, "Sur une nouvelle méthode de résolution du problème de la diffraction d'une onde plane par un réseau infiniment conducteur," Optics Communications 3(1):48-52, 1971.

[10] W. C. Meecham, "Variational method for the calculation of the distribution of energy reflected from a periodic surface. I." J. Appl. Phys. 27(4):361-367, 1956.

[11] H. A. Kalhor, "Numerical integral-equation analysis of scattering from diffraction gratings," Dissertation, University of California at Berkeley, 1970.

[12] W. C. Meecham and C. W. Peters, "Reflection of plane-polarized, electromagnetic radiation from an echelette diffraction grating," J. Appl. Phys. 28(2):216-217, 1957.

[13] R. Petit, "Diffraction d'une onde plane par un réseau métallique," Revue d'Optique 45(6): 249-276, 1966.

[14] N. K. Sheridon, "Production of blazed holograms," Appl. Phys. Letters 12(9):316-318, 1968.

[15] A. Hessel and J. Shmoys, "Bragg-angle blazing of diffraction gratings," J. Opt. Soc. Am. 62(5):742-743, 1972.